Structural and Multidisciplinary Optimization (2018) 58:245–263
https://doi.org/10.1007/s00158-017-1891-1

RESEARCH PAPER

On the ensemble of metamodels with multiple regional optimized weight factors

Hanfeng Yin[1] · Hongbing Fang[2] · Guilin Wen[1] · Matthew Gutowski[2] · Youye Xiao[1]

Received: 19 December 2016 / Revised: 11 October 2017 / Accepted: 25 December 2017 / Published online: 23 January 2018

Abstract
Metamodels are often used as surrogates for expensive high fidelity computational simulations (e.g., finite element analysis). Ensemble of metamodels (EM), which combines various types of individual metamodels in the form of a weighted average ensemble, is found to have improved accuracy over the individual metamodels used alone. Currently, there are mainly two kinds of EMs called as pointwise EM and average EM. The pointwise EM generally has better prediction accuracy than the average EM, but it is much more time-consuming than the average EM. In most cases, as a metamodel, EM is often used in the engineering design optimization which needs to invoke EM tens of thousands of times. Therefore, the average EM is still the most extensively used EM. To the authors' best knowledge, the most accurate average EM is the EM with optimized weight factors proposed by Acar et al. However, the EM proposed by Acar et al. is often too "rigid" and may not have sufficient accuracy over some regions of the design space. In order to deal with this problem and further improve the prediction accuracy, a new EM with multiple regional optimized weight factors (EM-MROWF) is proposed in this study. In this new EM, the design space is divided into multiple subdomains each of which is assigned a set of optimized weight factors. This new EM was constructed by combining three typical individual metamodels, i.e., polynomial regression (PR), radial basis function (RBF), and Kriging (KRG). The proposed technique was evaluated by ten benchmark problems and two engineering application problems. The ten benchmark problems are typical mathematical functions for evaluating the approximation performance in previous studies. And, the two engineering application problems refer to the vehicular passive safety in the field of crashworthiness design. The study results showed that the EM-MROWF performed much better than the other existing average EMs as well as the three individual metamodels.

Keywords Metamodel · Surrogate model · Approximate model · Ensemble · Optimization

1 Introduction

The design of modern engineering systems often relies on high-fidelity numerical simulations (e.g. finite element analysis) that are usually computationally expensive. In the optimum design of an engineering system, the high-fidelity numerical simulations are performed many times and thus the computational cost often becomes excessive and unaffordable. To reduce the computational cost, metamodels are used in the optimization work as the surrogates of the high-fidelity numerical simulations.

During the past decades, a large number of metamodeling methods have been proposed by the researchers and are available from literature. The commonly used metmodeling methods include polynomial regression (PR) (Box et al. 1978; Myers and Montgomery 2002), radial basis function (RBF) (Dyn et al. 1986; Buhmann 2003), Kriging (KRG) (Sacks et al. 1989; Simpson et al. 2001), Gaussian process (GP) (MacKay 1998; Rasmussen and Williams 2006), neural networks (Bishop 1995; Smith 1993), support vector regression (SVR) (Clarke et al. 2005; Gunn 1997) and multivariate adaptive regression splines (MARS) (Jerome 1990; Diana et al. 2015). In the work of Hou et al. (2007), they compared different PR models with different polynomial functions in the design optimization of hexagonal

✉ Guilin Wen
glwen@hnu.edu.cn

[1] State Key Laboratory of Advanced Design and Manufacturing for Vehicle Body, Hunan University, Changsha, Hunan 410082, People's Republic of China

[2] Department of Mechanical Engineering and Engineering Science, The University of North Carolina at Charlotte, Charlotte, NC 28223, USA

thin-walled structures. They found that quadratic polynomials provided the best approximations to the specific energy absorption (SEA) and maximum peak load. Fang et al. (2005) compared PR and several RBF models for the crashworthiness optimization problems and showed that the RBF models were more suitable for modeling highly nonlinear responses than the PR models. Song et al. (2013) carried out a comparative study on four commonly used metadmodels, PR, RBF, KRG and SVR, for the design optimization of foam-filled tapered structures. They found that no single model was the best for approximating all objective functions in the considered problems. Yin et al. (2011) employed PR, RBF, KRG, MARS and SVR models to approximate the responses of SEA and peak crushing stress of aluminum honeycomb structures. It was found that the best metamodels were different for the two responses. Forrester and Keane (2009) reviewed different metamodeling methods used in surrogate-based optimization and suggested that the choice of which surrogate to use should be based on the problem size, the expected complexity, and the cost of the analyses. From the available studies, the general consensus was that no single metamodel was the most effective for all problems. Different metamodels are suitable for fitting different functions; each metamodel has its advantages and drawbacks (Forrester and Keane 2009; Queipo et al. 2005; Wang and Shan 2007).

To improve the prediction accuracy of surrogate models, a number of studies were conducted on combining multiple metamodels into a single ensemble using the weighted sum approach (Goel et al. 2007; Zerpa et al. 2005; Sanchez et al. 2008; Acar and Rais-Rohani 2009; Acar 2010; Acar 2015; Lee and Dong-Hoon 2014; Fang et al. 2017; Ferreira and Serpa 2016; Zhou and Jiang 2016; Zhou et al. 2011; Zhang et al. 2012). Since an RBF could accurately capture the nonlinear aspect of a response, and a PR model could give the overall trend, an ensemble of metamodels (EM) of both RBF and PR models may have better prediction ability than the stand-alone models. In the work of Gu et al. (2015), they established the EM of PR, RBF, KRG and SVR for the responses of an occupant protection system. The results of the study showed that the EM had better prediction than all the individual metamodels.

In an EM, the weight factors have a significant effect on the prediction accuracy and there exist a number of methods for determining the weight factors such as the simple average weights (Goel et al. 2007), prediction-sum-of-squares-based average weights (Goel et al. 2007), optimized weights (Acar and Rais-Rohani 2009) and functional weights as the location of prediction point (Zerpa et al. 2005; Sanchez et al. 2008; Lee and Dong-Hoon 2014). Based on the method of determining the weight factors, EM can be classified into two types, an average EM and a pointwise EM (Lee and Dong-Hoon 2014). An average EM has unchanged weight factors in the entire design space, while a pointwise EM has varied weight factors which change as the location of a prediction point varies. The EMs proposed by Goel et al. (2007) and Acar and Rais-Rohani (2009) belong to average EM and the EMs proposed by Zerpa et al. (2005), Sanchez et al. (2008) and Lee and Dong-Hoon (2014) are typical pointwise EMs. The weight factors of the stand-alone metamodels in an average EM are determined based on their average accuracies throughout the entire design space, while the weight factors of the stand-alone metamodels in a pointwise EM are determined based on their accuracies at each prediction point. A pointwise EM was found to be more accurate than the average EM because it had varied weight factors according to the prediction point (Lee and Dong-Hoon 2014). However, it had much higher computational cost than the average EM especially when it was used as the surrogate in the design optimization.

In most cases, EM is employed as the surrogate of high fidelity computational simulation (e.g., finite element analysis) with expensive computational cost in the engineering design optimization (Hou et al. 2007; Fang et al. 2005; Song et al. 2013; Yin et al. 2011; Forrester and Keane 2009; Queipo et al. 2005; Wang and Shan 2007). Generally, the EM is invoked tens of thousands of times in the optimization process.

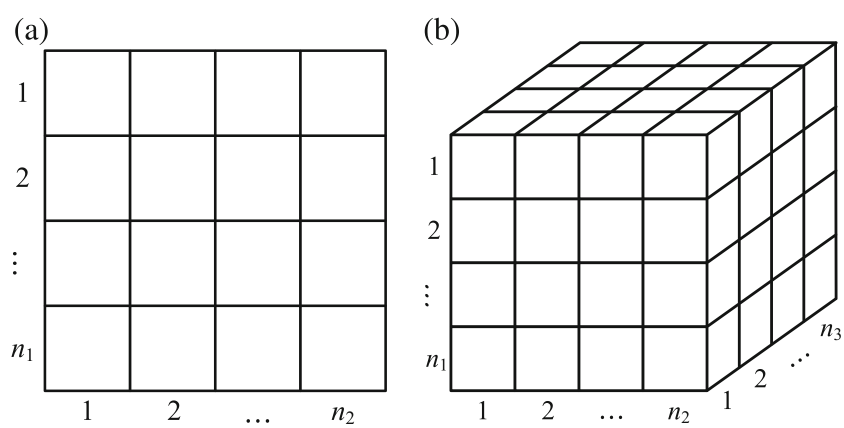

Fig. 1 Illustration of the divided regions in the design space: (**a**) two dimensions and (**b**) three dimensions

Fig. 2 The flowchart of the process of establishing the EM-MROWF

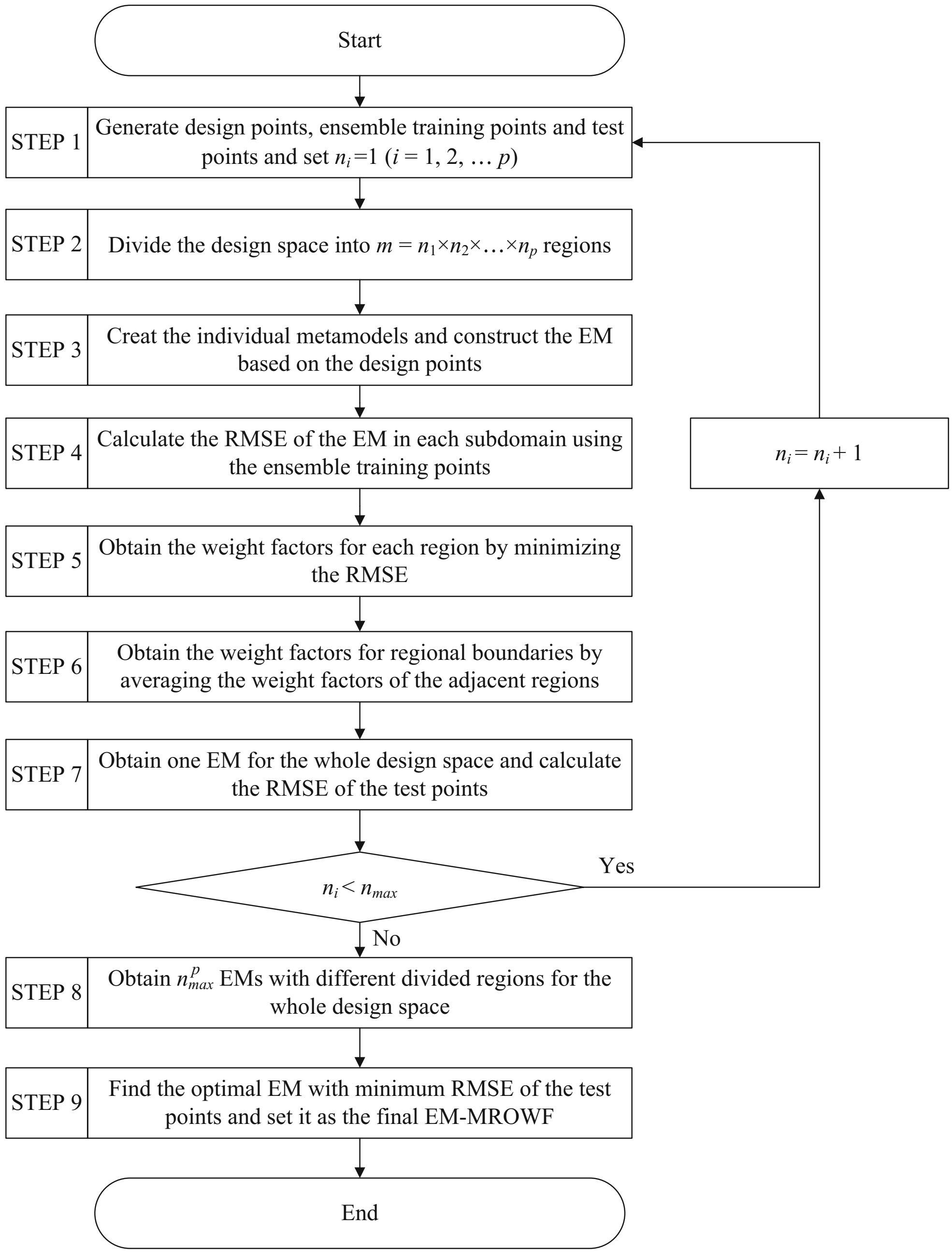

The computational time may not be accepted if we use pointwise EM in the practical design optimization. Thus, the average EM is relatively efficient in the practical design optimization. The average EM proposed by Acar et al. was found to be more accurate than the other existing average EMs (Acar and Rais-Rohani 2009). However, the average EM proposed by Acar et al. has only one set of weight factors across the entire design space, and this approach is often too "rigid" and may not have good prediction in some areas of the design space.

To deal with this issue and improve the accuracy of the EM proposed by Acar et al., a new EM with multiple regional optimized weight factors (EM-MROWF) was proposed and investigated in this study. In this new EM, the design space was divided into multiple subdomains, each of which had its own set of optimized weight factors. The optimized weight factors in each subdomain were determined by minimizing the error metric of the training points in that subdomain. The EM-MROWF technique was evaluated using ten benchmark problems and two engineering application problems. The results showed that the EM-MROWF had better prediction accuracy and robustness than the other two considered average EMs and the individual metamodels.

Table 1 User chosen functions and parameters of four individual metamodels (Yin et al. 2014)

Metamodel	Function	Parameters
PR	Cubic polynomial functions	–
RBF	$\phi(\|\mathbf{x}-\mathbf{x}_i\|)=\sqrt{\|\mathbf{x}-\mathbf{x}_i\|^2+c^2}$	$c = 1.0$
KRG	$R(\mathbf{x}_i,\mathbf{x}_j)=\prod_{k=1}^{n_{dv}}\exp\left(-\theta_k\left|x_k^i-x_k^j\right|^2\right)$	$0.01\le\theta_k\le 20$

2 Ensemble of metamodels

Metamodels are widely used in simulation-based design optimization to reduce the computational cost of a large number of expensive simulations. The most commonly used ensemble method is the weighted average ensemble (Goel et al. 2007) given by

$$\hat{y}_{\mathrm{ens}}(\mathbf{x})=\sum_{i=1}^{n_{\mathrm{M}}} w_i\hat{y}_i(\mathbf{x}) \tag{1}$$

where $\hat{y}_{\mathrm{ens}}$ is the prediction by the EM, $\mathbf{x}$ is the vector of design variables, n_{M} is the number of metamodels used in the ensemble, w_i is the weight factor of the ith basis metamodel in the ensemble, and $\hat{y}_i$ is the predicted value by the ith metamodel. To have unbiased response estimation, the following equation should be satisfied by the weight factors:

$$\sum_{i=1}^{n_{\mathrm{M}}} w_i=1 \tag{2}$$

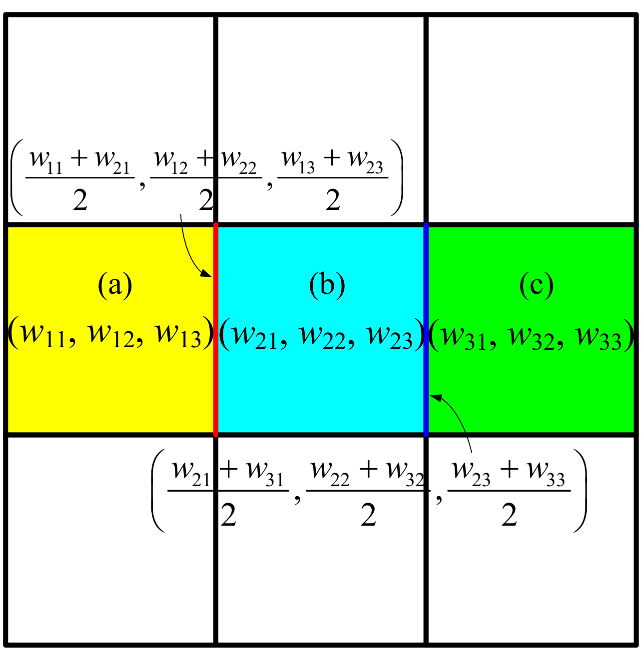

Fig. 3 Illustration of the weight calculation for the adjacent regions

A metamodel that is deemed more accurate should be assigned a large weight factor, and the less accurate model should have less influence on the predictions. There are many possible strategies of determining weight factors (Lee and Dong-Hoon 2014).

Among the existing EM, there are mainly two types of EMs, i.e., the pointwise EM (Zerpa et al. 2005; Sanchez et al. 2008; Lee and Dong-Hoon 2014) and the average EM (Goel et al. 2007; Acar and Rais-Rohani 2009). Generally, the accuracy of the pointwise EM is much better than that of the average EM, but the pointwise EM is much more time-consuming than the average EM. As a metamodel, the EM is often used as the surrogate of the numerical simulation (e.g., finite element analysis) for the engineering design optimization. In the design optimization process, the computational time will be exaggerated if we use pointwise EM as the surrogate of the numerical simulation. In order to consider the numerical cost of the EM, we only consider the average EM in this study.

2.1 The EM proposed by Goel

Goel et al. (2007) proposed an average EM using the basis metamodels of PR, KRG and RBF. The weight factors of the EM proposed by Goel were determined as:

$$w_i=\frac{w_i^*}{\sum_{i=1}^{M} w_i^*} \tag{3}$$

$$w_i^*=\left(E_i+\alpha E_{avg}\right)^{\beta},\beta<0,\alpha<1 \tag{4}$$

$$E_{avg}=\frac{\sum_{i=1}^{M} E_i}{M} \tag{5}$$

$$E_i=GMSE_i=\frac{1}{ndes}\sum_{k=1}^{ndes}\left[y(\mathbf{x}_k)-\hat{y}_i^{(-k)}(\mathbf{x}_k)\right]^2 \tag{6}$$

where M is the number of individual metamodels, $ndes$ is the number of design points, $\mathbf{x}_k$ is the kth design point, $y(\mathbf{x}_k)$ is the real response value at $\mathbf{x}_k$, and $\hat{y}_i^{(-k)}(\mathbf{x}_k)$ is the predicted response value of the ith basis metamodel generated using $nexp$-1 design points without the kth point at $\mathbf{x}_k$. In this study, $\alpha = 0.05$ and $\beta = -1$ as the Goel et al. suggested. In the method proposed by Goel et al.,

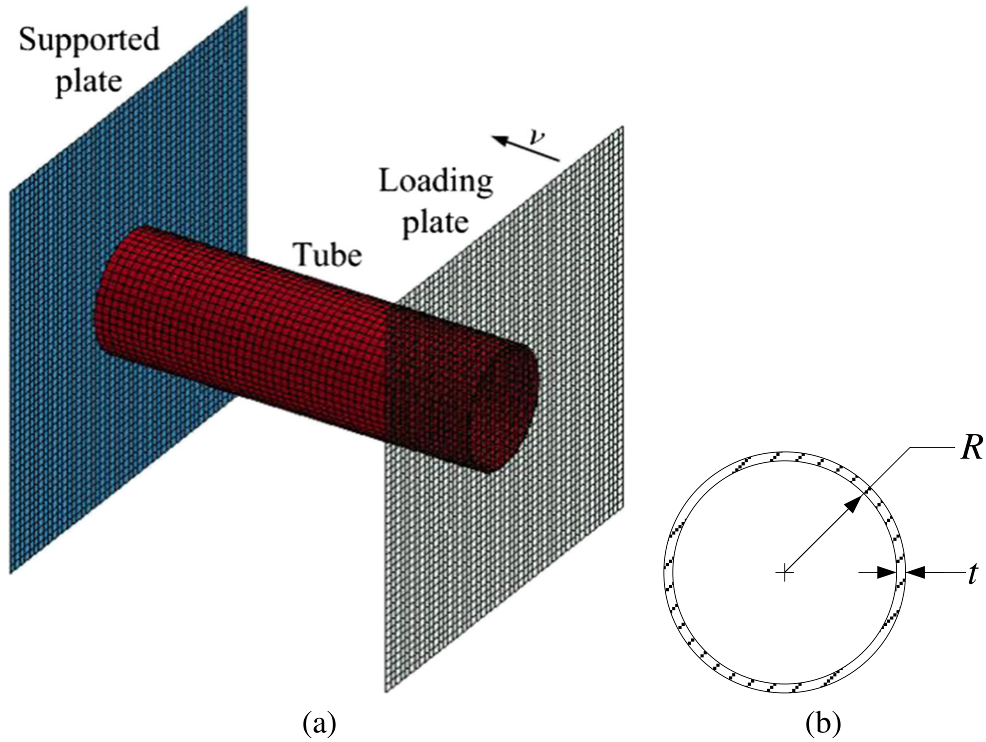

Fig. 4 FE model and illustration of design variables of the cylinder thin-walled column: (**a**) FE model and (**b**) illustration of design variables

the generalized mean square cross-validation error (GMSE) was used to calculate the prediction errors of the basis metamodel.

2.2 The EM proposed by Acar

An error-based minimization method (Acar and Rais-Rohani 2009; Acar 2010, 2015) is recognized as an effective method for determining the weight factors of the EM. Acar and Rais-Rohani (2009) proposed an ensemble of metamodels with optimized weight factors, in which they determined the weight factors w_i by solving an optimization problem as

$$\begin{cases} \text{Minimize Error}\left(\hat{y}_{\text{ens}}\right) \\ \text{s.t.} \quad \sum_{i=1}^{n_{\text{M}}} w_i = 1 \end{cases} \tag{7}$$

where Error($\hat{y}_{\text{ens}}$) is the selected error metric that measures the accuracy of the ensemble-predicted response $\hat{y}_{\text{ens}}$. In Acar and Rais-Rohani's study, GMSE was selected as the error metric to evaluate the accuracy of the ensemble of metamodels (Acar 2015). Then, GMSE was selected to evaluate the accuracy of the ensemble-predicted response $\hat{y}_{\text{ens}}$. The Error($\hat{y}_{\text{ens}}$) of (7) will be written as

$$\text{Error}\left(\hat{y}_{\text{ens}}\right) = GMSE_{\text{ens}} = \frac{1}{ndes} \sum_{k=1}^{ndes} \left[y(\mathbf{x}_k) - \hat{y}_{\text{ens}}^{(-k)}(\mathbf{x}_k) \right]^2 \tag{8}$$

Table 2 Responses of the design points for the thin-walled column crash problem

No.	*R* (mm)	*t* (mm)	EA (kJ)	PCF (kN)	SEA (kJ/kg)
1	79	2.85	8.739	134.44	11.4446
2	83	1.45	2.907	45.573	7.1219
3	95	1.35	2.7113	37.876	6.2327
4	99	1.85	4.9181	55.225	7.9165
5	75	2.45	6.7958	103.37	10.9055
6	81	1.95	4.8268	70.943	9.0103
7	69	2.95	8.7972	128.52	12.7452
8	91	1.75	4.3508	65.176	8.0549
9	61	2.15	5.1846	73.361	11.6602
10	67	1.25	2.2375	28.21	7.8788
11	87	1.05	1.8314	27.5	5.9109
12	63	1.65	3.3225	46.272	9.4268
13	93	2.25	6.3145	106.21	8.8968
14	85	2.35	6.5542	106.07	9.6743
15	89	2.75	8.7528	139.47	10.5438
16	73	1.55	3.3476	44.262	8.7242
17	77	1.15	2.0095	24.831	6.6915
18	71	2.05	4.9883	72.46	10.1064
19	97	2.65	9.135	129.47	10.4771
20	65	2.55	7.0502	99.915	12.5444

Table 3 Responses of the test points for the thin-walled column crash problem

No.	R (mm)	t (mm)	EA (kJ)	PCF (kN)	SEA (kJ/kg)
1	73.79	1.31	2.3797	34.5630	7.2387
2	94.08	2.64	8.1013	136.1800	9.6245
3	87.99	1.76	4.0882	63.8470	7.7824
4	80.45	2.05	5.1393	78.0010	9.2399
5	96.37	1.46	3.0392	41.9080	6.3928
6	68.26	2.29	5.7388	87.6090	10.8682
7	91.83	1.68	3.8887	57.4820	7.4177
8	89.20	2.39	6.8776	112.5400	9.5328
9	75.48	2.48	6.7731	103.4600	10.7376
10	82.40	2.58	7.6675	119.6200	10.6861
11	65.14	1.96	4.4404	66.0820	10.2791
12	62.18	1.20	2.0742	24.1870	8.2225
13	79.64	1.51	3.0533	48.2830	7.4526
14	93.47	2.81	8.9713	147.4300	10.1211
15	99.71	1.25	2.3973	26.9210	5.6540
16	67.73	2.75	7.7750	115.7500	12.2614
17	84.26	2.17	5.6086	88.0930	9.0721
18	76.84	2.91	8.9568	135.7500	11.7868
19	60.90	1.06	1.6707	20.2880	7.6208
20	71.71	1.89	4.3304	67.5830	9.3838

Table 4 Responses of the design points for the airbag cushion problem

No.	λ	A (mm^2)	a_{peak} (mm/ms^2)
1	0.975	537.333	2.5755
2	1.075	31.793	2.9792
3	1.375	19.233	3.5447
4	1.475	113.433	3.5701
5	0.875	330.093	2.3267
6	1.025	141.693	2.8853
7	0.725	596.993	1.7822
8	1.275	88.313	3.2267
9	0.525	207.633	1.0548
10	0.675	9.813	1.7974
11	1.175	0.393	3.0983
12	0.575	66.333	1.3687
13	1.325	245.313	3.2610
14	1.125	286.133	2.9033
15	1.225	480.813	3.0281
16	0.825	47.493	2.2632
17	0.925	3.533	2.4965
18	0.775	173.093	2.1010
19	1.425	427.433	3.3293
20	0.625	377.193	1.4210

where $ndes$ is the number of design points, $\mathbf{x}_k$ is the kth design point, $y(\mathbf{x}_k)$ is the real response value at $\mathbf{x}_k$, and $\hat{y}_{\text{ens}}^{(-k)}(\mathbf{x}_k)$ is the predicted response value of the ensemble metamodel generated using $nexp$-1 design points at $\mathbf{x}_k$.

3 New proposed ensemble of metamodels

In this study, a new EM approach was investigated by dividing the design space into multiple subdomains and use a set of optimized weight factors for each subdomain. The basic idea of the new EM approach was to allow the subdomain to have independently determined sets of weight factors so that they will not affect or be affected by those of other subdomains. With multiple regional optimized weight factors, the accuracy of the EM could be improved in each of the subdomains and thus across the entire design space.

The first step of constructing the EM with multiple regional optimized weight factors was to divide the design space into $m = n_1 \times n_2 \times \cdots \times n_p$ subdomains or regions (see Fig. 1), where n_i is the number of sections of ith variable, and p is the number of variables. In each region, there is one set of weight factors that is obtained by minimizing the GMSE on the design points in that region. The flowchart of the process to establish the EM-MROWF is shown in Fig. 2 and a detailed description is given as follows.

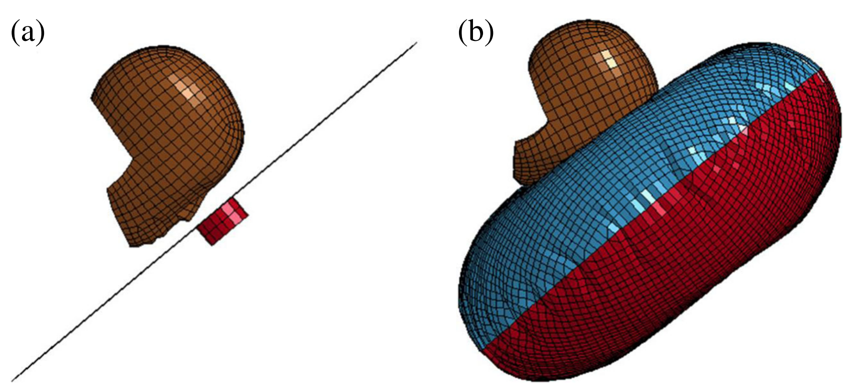

Fig. 5 FE models of the airbag cushion system: (**a**) before airbag deployment and (**b**) after airbag deployment

Table 5 Responses of the test points for the airbag cushion problem

No.	λ	A (mm^2)	a_{peak} (mm/ms^2)
1	0.718	470.291	1.8153
2	1.046	30.997	2.8403
3	0.546	116.211	1.2238
4	1.111	13.556	3.1062
5	0.955	274.379	2.4650
6	0.673	0.689	1.7366
7	0.845	531.085	2.1401
8	1.409	82.722	3.4479
9	1.283	54.563	3.3197
10	1.085	221.287	2.8429
11	1.463	327.841	3.4961
12	0.599	66.634	1.4815
13	1.398	573.323	3.3091
14	1.317	233.719	3.2606
15	1.170	134.788	3.0865
16	0.774	24.479	2.0766
17	1.214	187.461	3.0873
18	0.915	5.736	2.5118
19	0.611	362.812	1.4428
20	0.886	404.788	2.3469

STEP 1: Generate *ndes* design points using the optimal Latin hypercube sampling, and create *ntest* test points using the regular Latin hypercube sampling. The design points were used to create the individual metamodels, i.e., PR, RBF and KRG. The ensemble training points were used to calculate the weight factors of the ensemble of metamodels. The test points were used to calculate the root mean square error (RMSE) and maximum absolute relative error (MARE) of the ensemble of metamodels.
STEP 2: Divide the design space into $m = n_1 \times n_2 \times \cdots \times n_p$ regions, as illustrated in Fig. 1.

STEP 3: Create the individual metamodels, i.e., PR, RBF and KRG, and construct the EM based on the design points. The functions and parameters of these metamodels are given in Table 1.
STEP 4: Calculate the error metric GMSE of the EM in each subdomain using the design points in that region.
STEP 5: Obtain the optimized weight factors for each region by minimizing the GMSE. In this study, the sequential quadratic programming (SQP) optimizer of MATLAB, the "fmincon" function, was used to solve the optimization problem of (7). A total of $m = n_1 \times n_2 \times \cdots \times n_p$ sets of optimized weight factors were obtained for the $m = n_1 \times n_2 \times \cdots \times n_p$ regions.
STEP 6: Obtain the weight factors for the regional boundaries by averaging the weight factors of the adjacent regions. The weight factors for the regional boundaries were determined by averaging the weight factors of the adjacent regions, which is illustrated in Fig. 3 (e.g. if the weight factors of region A and region B were (w_{11}, w_{12}, w_{13}) and (w_{21}, w_{22}, w_{23}), respectively. The weight factors of the boundary of region A and region B would be ($w_{11}/2 + w_{21}/2$, $w_{12}/2 + w_{22}/2$, $w_{13}/2 + w_{23}/2$).)
STEP 7: Obtain one EM for the whole design space and calculate the RMSE and MARE of the test points. RMSE and MARE can be calculated as:

$$RMSE = \sqrt{\frac{1}{ntest}\sum_{i=1}^{ntest}\left[y(\mathbf{x}_i) - \hat{y}(\mathbf{x}_i)\right]^2}, \tag{9}$$

$$MARE = \max\left(\left|\frac{y(\mathbf{x}_i) - \hat{y}(\mathbf{x}_i)}{y(\mathbf{x}_i)}\right|\right), \tag{10}$$

where *ntest* is the number of test points, $\mathbf{x}_i$ is the ith design point, $y(\mathbf{x}_i)$ is the real response value at $\mathbf{x}_i$, and $\hat{y}(\mathbf{x}_i)$ is the

Table 6 Summary of the *ndes*, *ntest* and *ntotal** for the benckmark problems

ID	Problem	*nvar*	*ndes*	*ntest*	*ntotal*
1	Branin-Hoo	2	20, 30, 40, 50, 60	1000	1020, 1030, 1040, 1050, 1060
2	Camelback	2	20, 30, 40, 50, 60	1000	1020, 1030, 1040, 1050, 1060
3	Goldstein-price	2	20, 30, 40, 50, 60	1000	1020, 1030, 1040, 1050, 1060
4	2D multi-modal	2	20, 30, 40, 50, 60	1000	1020, 1030, 1040, 1050, 1060
5	Haupt	2	20, 30, 40, 50, 60	1000	1020, 1030, 1040, 1050, 1060
6	Crane	2	20, 30, 40, 50, 60	1000	1020, 1030, 1040, 1050, 1060
7	Peak	2	20, 30, 40, 50, 60	1000	1020, 1030, 1040, 1050, 1060
8	Waving	2	20, 30, 40, 50, 60	1000	1020, 1030, 1040, 1050, 1060
9	Rastrigin	2	20, 30, 40, 50, 60	1000	1020, 1030, 1040, 1050, 1060
10	Rosenbrock	2	20, 30, 40, 50, 60	1000	1020, 1030, 1040, 1050, 1060

* *ndes* and *ntest* denote the numbers of the design points and test points, respectively. *Ntotal* represents the total sampling points which equals to *ndes* + *ntest*

Table 7 Normalized RMSE values with *ndes* = 20 for Test 1

ID	Problem	*ndes*	EM-MROWF	GOEL	ACAR	PRS	RBF	KRG
1	Branin-Hoo	20	**1.0000**	1.0811	**1.0000**	1.5370	3.1506	1.0348
2	Camelback	20	**1.0000**	1.1157	**1.0000**	2.5324	1.1967	1.1901
3	Goldstein-price	20	1.0567	**1.0000**	1.2422	1.6521	1.0784	1.3392
4	2D multi-modal	20	**1.0000**	1.1906	**1.0000**	7.7781	3.1063	**1.0000**
5	Haupt	20	1.0609	**1.0000**	1.0609	1.0702	2.1813	1.1706
6	Crane	20	1.0293	1.2326	1.0293	1.5678	2.9483	**1.0000**
7	Peak	20	1.2292	1.2825	1.2319	2.2085	2.3040	**1.0000**
8	Waving	20	1.1254	**1.0000**	1.1447	1.1447	2.3316	1.1982
9	Rastrigin	20	1.5223	1.2797	1.5223	**1.0000**	1.6805	1.0218
10	Rosenbrock	20	1.0505	1.2949	1.2531	3.1969	1.6016	**1.0000**
Average			1.1074	1.1477	1.1484	2.3688	2.1579	1.0955
Standard deviation			0.1536	0.1171	0.1595	1.9211	0.7203	0.1141

The symbol bold represents the best value which is normalized to 1 in each case.

predicted response value of the ensemble metamodel at $\mathbf{x}_i$. Generally, RMSE and MARE are used to evaluate the global and local errors of the metamodel, respectively (Jin et al. 2001).

STEP 8: Obtain ${n_{\max}}^p$ EMs with differently divided regions for the whole design space. In this study, in order to save the computational cost, $n_{\max}$ was chosen as four.
STEP 9: Find the best EM with minimum RMSE of the test points and set it as the final EM-MROWF.

4 Example problems

Ten mathematical benchmark problems and two engineering application problems were used to test the performance of the proposed EM-MROWF technique. The first engineering application was a cylindrical thin-walled column crushed by a dynamic axial load, and the second application was an airbag cushion impacted by a dummy head. For both application problems, the responses were obtained using nonlinear finite element (FE) simulations.

4.1 Benchmark problems

The ten benchmark problems (Acar 2015; Lee and Dong-Hoon 2014; Wikipedia 2015) used in this study are given as follows.

(1) Branin-Hoo function

$$y(x_1,x_2)=\left(x_2-\frac{5.1x_1^2}{4\pi^2}+\frac{5x_1}{\pi}-6\right)^2+10\left(1-\frac{1}{8\pi}\right)\cos(x_1)+10 \quad (11)$$

Table 8 Normalized RMSE values with *ndes* = 30 for Test 1

ID	Problem	*ndes*	EM-MROWF	GOEL	ACAR	PRS	RBF	KRG
1	Branin-Hoo	30	**1.0000**	1.3376	1.3772	4.8833	3.8906	1.4756
2	Camelback	30	1.6305	1.6233	1.7020	9.0444	**1.0000**	2.2491
3	Goldstein-price	30	**1.0000**	1.4566	**1.0000**	2.6726	**1.0000**	2.1721
4	2D multi-modal	30	**1.0000**	1.7101	**1.0000**	28.6957	4.7536	**1.0000**
5	Haupt	30	1.4846	1.7158	1.5397	3.1958	2.9730	**1.0000**
6	Crane	30	1.0058	1.0628	1.0058	1.4079	2.3466	**1.0000**
7	Peak	30	1.3707	1.3779	1.7984	1.9691	3.3994	**1.0000**
8	Waving	30	**1.0000**	1.0292	1.1747	1.1747	2.9841	1.1104
9	Rastrigin	30	1.0911	1.0744	1.1334	**1.0000**	1.3239	1.1334
10	Rosenbrock	30	**1.0000**	10.0361	**1.0000**	391.2876	37.8470	**1.0000**
Average			1.1583	2.2424	1.2731	44.5331	6.1518	1.3141
Standard deviation			0.2297	2.6095	0.2943	115.8571	10.6313	0.4695

The symbol bold represents the best value which is normalized to 1 in each case.

Table 9 Normalized RMSE values with $ndes = 40$ for Test 1

ID	Problem	*ndes*	EM-MROWF	GOEL	ACAR	PRS	RBF	KRG
1	Branin-Hoo	40	1.0828	1.8451	1.0828	25.7168	14.1362	**1.0000**
2	Camelback	40	**1.0000**	1.1917	1.0229	8.3381	1.0263	2.7807
3	Goldstein-price	40	**1.0000**	1.4307	1.1069	7.2046	11.0691	1.5345
4	2D multi-modal	40	**1.0000**	10.1842	**1.0000**	291.6117	21.2290	**1.0000**
5	Haupt	40	**1.0000**	1.7031	1.0629	6.7354	7.9061	1.0977
6	Crane	40	1.0667	1.0533	1.0667	1.2362	4.5219	**1.0000**
7	Peak	40	1.1112	1.6529	1.1112	3.8730	9.0369	**1.0000**
8	Waving	40	1.5925	1.6247	1.8445	1.2288	3.2175	**1.0000**
9	Rastrigin	40	1.0304	1.0476	1.0463	**1.0000**	2.8663	1.1957
10	Rosenbrock	40	**1.0000**	23.4864	**1.0000**	674.5060	54.9614	**1.0000**
Average			1.0884	4.5220	1.1344	102.1451	12.9971	1.2609
Standard deviation			0.1725	6.8425	0.2396	208.9274	15.1287	0.5314

The symbol bold represents the best value which is normalized to 1 in each case.

where $x_1 \in [-5, 10]$ and $x_2 \in [0, 15]$.

(2) Camelback function

$$y(x_1, x_2) = \left(4 - 2.1x_1^2 + \frac{x_1^4}{3}\right)x_1^2 + x_1x_2 + \left(-4 + 4x_2^2\right)x_2^2 \tag{12}$$

where $x_1, x_2 \in [-2, 2]$.

(3) Goldstein-price function

$$y(x_1, x_2) = \left[1 + (x_1 + x_2 + 1)^2 \times \left(19 - 4x_1 + 3x_1^2 - 14x_2 + 6x_1x_2 + 3x_2^2\right)\right] \times \left[30 + (2x_1 - 3x_2)^2 \times \left(18 - 32x_1 + 12x_1^2 + 48x_2 - 36x_1x_2 + 27x_2^2\right)\right] \tag{13}$$

where $x_1, x_2 \in [-2, 2]$.

(4) 2D multi-modal function

$$y(x_1, x_2) = x_1x_2\sin(x_1) + \left(x_1^2/10\right) + x_1 - 1.5x_2 \tag{14}$$

where $x_1, x_2 \in [-2, 2]$.

(5) Haupt function

$$y(x_1, x_2) = x_1\sin(4x_1) + 1.1x_2\sin(2x_2) \tag{15}$$

where $x_1, x_2 \in [0, 4]$.

(6) Crane function

$$y(x_1, x_2) = e^{\cos(x_1 - x_2)}\sin\left\{\left[\cos^2(x_1 - x_2) + x_1 + x_2\right] / \left[1 + (x_1 - x_2)^2\right]\right\} \tag{16}$$

where $x_1, x_2 \in [-4, 4]$.

(7) Peak function

$$y(x_1, x_2) = 3\left(1 - x_1^2\right)e^{-x_1^2 - (x_2+1)^2} - 10\left(\frac{x_1}{5} - x_1^3 - x_2^5\right) e^{-x_1^2 - x_2^2} - \frac{1}{3}e^{-(x_1+1)^2 - x_2^2} \tag{17}$$

where $x_1, x_2 \in [-3, 3]$.

Table 10 Normalized RMSE values with $ndes = 50$ for Test 1

ID	Problem	*ndes*	EM-MROWF	GOEL	ACAR	PRS	RBF	KRG
1	Branin-Hoo	50	**1.0000**	3.5345	**1.0000**	40.1539	24.2682	1.0006
2	Camelback	50	**1.0000**	1.3856	**1.0000**	20.7263	**1.0000**	5.2628
3	Goldstein-price	50	**1.0000**	2.0576	**1.0000**	14.5952	**1.0000**	3.3529
4	2D multi-modal	50	**1.0000**	29.3087	1.0004	1283.8484	47.1488	1.0004
5	Haupt	50	**1.0000**	1.2907	**1.0000**	11.8416	14.8758	1.6112
6	Crane	50	**1.0000**	1.0376	1.0303	1.2509	2.1503	1.0122
7	Peak	50	1.3836	2.3486	1.5294	5.1491	7.8747	**1.0000**
8	Waving	50	**1.0000**	1.2222	1.2954	1.8332	1.8340	1.2541
9	Rastrigin	50	1.0673	**1.0000**	1.0858	1.0072	3.3176	1.0873
10	Rosenbrock	50	**1.0000**	41.4273	**1.0000**	1232.0237	73.6073	**1.0000**
Average			1.0451	8.4613	1.0941	261.2430	17.7077	1.7581
Standard deviation			0.1146	13.7430	0.1695	498.6079	23.2350	1.3567

The symbol bold represents the best value which is normalized to 1 in each case.

Table 11 Normalized RMSE values with $ndes = 60$ for Test 1

ID	Problem	*ndes*	EM-MROWF	GOEL	ACAR	PRS	RBF	KRG
1	Branin-Hoo	60	**1.0000**	9.5172	**1.0000**	316.4286	43.3892	**1.0000**
2	Camelback	60	**1.0000**	2.4597	**1.0000**	58.1528	**1.0000**	8.4289
3	Goldstein-price	60	1.4599	1.5373	1.4599	15.3353	**1.0000**	1.9170
4	2D multi-modal	60	1.1042	110.1322	1.1042	7631.7507	122.3691	**1.0000**
5	Haupt	60	**1.0000**	1.4164	1.0552	24.8754	7.6530	1.0363
6	Crane	60	1.0177	1.0854	1.0177	1.4154	5.7436	**1.0000**
7	Peak	60	**1.0000**	2.1889	1.1048	6.8066	15.6973	1.1024
8	Waving	60	**1.0000**	1.6686	2.0110	2.6726	4.2353	1.8149
9	Rastrigin	60	1.0002	**1.0000**	1.0002	1.0252	7.5979	1.0978
10	Rosenbrock	60	**1.0000**	99.1707	**1.0000**	7510.5305	120.0976	**1.0000**
Average			1.0582	23.0176	1.1753	1556.8993	32.8783	1.9397
Standard deviation			0.1374	40.9592	0.3085	3008.6002	45.7013	2.1882

The symbol bold represents the best value which is normalized to 1 in each case.

Table 12 Summarized normalized average RMSE values for all benchmark problems

ndes	*ntest*	*ntotal*	EM-MROWF	GOEL	ACAR	PRS	RBF	KRG
20	1000	1020	1.0109	1.0476	1.0483	2.1623	1.9698	**1.0000**
30	1000	1030	**1.0000**	1.9359	1.0991	38.4469	5.3111	1.1345
40	1000	1040	**1.0000**	4.1547	1.0423	93.8489	11.9415	1.1585
50	1000	1050	**1.0000**	8.0962	1.0469	249.9694	16.9435	1.6822
60	1000	1060	**1.0000**	21.7517	1.1107	1471.2713	31.0700	1.8330
Average			1.0022	7.3972	1.0694	371.1398	13.4472	1.3616
Standard deviation			0.0043	7.5788	0.0292	556.5412	10.2273	0.3312

The symbol bold represents the best value which is normalized to 1 in each case.

(8) Waving function

$$y(x_1,x_2) = 2 + 0.01\left(x_2 - x_1^2\right)^2 + (1-x_1)^2 + 2\left(2-x_2^2\right) + 7\sin(0.5x_1)\sin(0.7x_1x_2) \quad (18)$$

where $x_1, x_2 \in [0, 5]$.

(9) Rastrigin function

$$y(x_1,x_2) = x_1^2 + x_2^2 - \cos(18x_1) - \cos(18x_2) \quad (19)$$

where $x_1, x_2 \in [-1, 1]$.

Table 13 Normalized MARE values with $ndes = 20$ for Test 1

ID	Problem	*ndes*	EM-MROWF	GOEL	ACAR	PRS	RBF	KRG
1	Branin-Hoo	20	**1.0000**	1.4260	1.2740	3.8456	8.2069	1.5332
2	Camelback	20	1.0155	**1.0000**	4.0458	23.3617	1.5664	5.9017
3	Goldstein-price	20	**1.0000**	5.4042	7.0789	12.9064	1.2092	**1.0000**
4	2D multi-modal	20	1.9506	**1.0000**	1.9506	30.0819	4.1822	1.9506
5	Haupt	20	1.1896	**1.0000**	1.1896	1.7272	3.1093	1.3231
6	Crane	20	**1.0000**	3.4849	1.7327	9.5128	43.5543	1.5093
7	Peak	20	10.4837	14.4376	14.7119	40.2929	36.2147	**1.0000**
8	Waving	20	1.6658	2.5173	2.9694	2.9694	**1.0000**	1.2312
9	Rastrigin	20	1.5080	1.5404	1.6455	**1.0000**	1.8004	1.5156
10	Rosenbrock	20	1.0779	5.4602	3.3756	43.7483	8.8033	**1.0000**
Average			2.1891	3.7271	3.9974	16.9446	10.9647	1.7965
Standard deviation			2.7830	3.9299	3.9483	15.4970	14.7865	1.3984

The symbol bold represents the best value which is normalized to 1 in each case.

Table 14 Normalized MARE values with $ndes = 30$ for Test 1

ID	Problem	*ndes*	EM-MROWF	GOEL	ACAR	PRS	RBF	KRG
1	Branin-Hoo	30	**1.0000**	1.2597	1.4023	7.9394	6.9846	2.0177
2	Camelback	30	**1.0000**	1.5615	**1.0000**	50.9719	0.2349	1.4008
3	Goldstein-price	30	**1.0000**	8.7442	**1.0000**	33.2038	**1.0000**	8.2540
4	2D multi-modal	30	**1.0000**	2.9029	**1.0000**	78.0319	6.1115	**1.0000**
5	Haupt	30	**1.0000**	1.5815	1.0626	1.2444	15.1943	1.2645
6	Crane	30	1.0104	17.9619	26.4215	23.8980	414.4597	**1.0000**
7	Peak	30	7.5540	41.1055	63.6183	66.1785	192.4292	**1.0000**
8	Waving	30	10.3375	10.5862	10.3375	10.3375	**1.0000**	14.6854
9	Rastrigin	30	1.2139	1.3709	1.4906	**1.0000**	1.4353	1.5682
10	Rosenbrock	30	**1.0000**	37.7751	**1.0000**	2105.9653	46.5476	**1.0000**
Average			2.6116	12.4849	10.8333	237.8771	68.5397	3.3191
Standard deviation			3.2283	14.4425	19.2041	623.2293	128.1861	4.3327

The symbol bold represents the best value which is normalized to 1 in each case.

(10) Rosenbrock function

$$y(\mathbf{x}) = \sum_{i=1}^{n-1}\left[100\left(x_{i+1}-x_i^2\right)^2 + (x_i-1)^2\right] \tag{20}$$

where $x_i \in [-2, 2]$, $i = 1, 2$.

4.2 Engineering application problems

4.2.1 Thin-walled column crushing problem

Thin-walled columns are widely used as energy absorbers in engineering applications. In this study, the FE model of a cylindrical thin-walled column, as shown in Fig. 4a, was created for LS-DYNA (Hallquist 1998a, b) and used to simulate axial crushing of the column under dynamic loading conditions. As an energy absorber, the energy absorption (EA), peak crushing force (PCF), and specific energy absorption (SEA) are three important indicators for evaluating the energy absorption capacity and efficiency. The EA is calculated by

$$\mathrm{EA} = \int_0^d F(x)dx \tag{21}$$

where d is the crushing distance and F is the crushing force. The SEA is defined as (Kim 2002)

$$\mathrm{SEA} = \frac{\mathrm{EA}}{M} \tag{22}$$

where M is the mass of the structure.

The three performance indicators did not have explicit mathematical formulas and thus metamodels needed to be established using FE simulation results. The design variables of the cylinder thin-walled column were the radius

Table 15 Normalized MARE values with $ndes = 40$ for Test 1

ID	Problem	*ndes*	EM-MROWF	GOEL	ACAR	PRS	RBF	KRG
1	Branin-Hoo	40	1.0057	9.6582	1.7915	213.9820	46.1504	**1.0000**
2	Camelback	40	**1.0000**	11.1181	2.7318	247.3032	4.7649	107.3323
3	Goldstein-price	40	**1.0000**	1.7002	3.3168	27.6370	3.3168	4.6276
4	2D multi-modal	40	**1.0000**	74.2188	**1.0000**	5320.0000	61.7188	**1.0000**
5	Haupt	40	**1.0000**	1.1353	1.0509	3.2309	6.4784	**1.0000**
6	Crane	40	**1.0000**	1.9308	2.6493	4.1484	8.1179	1.1288
7	Peak	40	1.1364	8.8221	3.7487	36.1953	145.9479	**1.0000**
8	Waving	40	1.0352	3.8735	3.6900	9.7898	**1.0000**	1.6054
9	Rastrigin	40	**1.0000**	1.0815	1.0584	**1.0000**	1.9940	1.1089
10	Rosenbrock	40	**1.0000**	47.9086	**1.0000**	2821.0216	49.4289	**1.0000**
Average			1.0177	16.1447	2.2037	868.4308	32.8918	12.0803
Standard deviation			0.0409	23.4860	1.0964	1697.8807	43.6015	31.7685

The symbol bold represents the best value which is normalized to 1 in each case.

Table 16 Normalized MARE values with *ndes* = 50 for Test 1

ID	Problem	*ndes*	EM-MROWF	GOEL	ACAR	PRS	RBF	KRG
1	Branin-Hoo	50	**1.0000**	5.6621	**1.0000**	36.4582	39.6996	1.0246
2	Camelback	50	**1.0000**	11.4871	1.0821	355.7157	1.0821	154.0538
3	Goldstein-price	50	**1.0000**	1.0693	2.1759	19.8773	2.1759	2.2637
4	2D multi-modal	50	**1.0000**	66.0556	1.3889	7773.2222	27.5000	1.3889
5	Haupt	50	**1.0000**	1.0859	1.0177	4.2393	13.3411	1.0556
6	Crane	50	**1.0000**	11.4605	7.7727	7.9709	102.3860	2.4104
7	Peak	50	1.1199	12.3005	5.9937	33.3052	77.9452	**1.0000**
8	Waving	50	4.3332	23.8994	25.8497	41.4823	7.6345	**1.0000**
9	Rastrigin	50	**1.0000**	1.0500	1.0858	1.1114	2.1304	1.0876
10	Rosenbrock	50	**1.0000**	126.9953	1.1251	15,860.8187	26.5614	1.1251
Average			1.3453	26.1066	4.8492	2413.4201	30.0456	16.6410
Standard deviation			0.9966	38.3365	7.3601	5038.5887	32.8869	45.8070

The symbol bold represents the best value which is normalized to 1 in each case.

Table 17 Normalized MARE values with *ndes* = 60 for Test 1

ID	Problem	*ndes*	EM-MROWF	GOEL	ACAR	PRS	RBF	KRG
1	Branin-Hoo	60	**1.0000**	6.6738	1.2688	885.6810	66.7563	1.2688
2	Camelback	60	**1.0000**	4.1925	1.0009	407.7011	1.0009	9.5742
3	Goldstein-price	60	**1.0000**	3.3120	3.5742	74.0009	**1.0000**	1.8666
4	2D multi-modal	60	1.3926	622.5904	2.4795	74,897.0552	75.0554	**1.0000**
5	Haupt	60	**1.0000**	1.1448	4.5812	19.9271	72.1765	4.5407
6	Crane	60	1.2725	13.0926	1.2725	**1.0000**	1558.7820	14.6677
7	Peak	60	2.7182	33.4037	4.2566	87.6442	527.4450	**1.0000**
8	Waving	60	1.4432	54.0901	62.8965	87.5623	**1.0000**	10.4344
9	Rastrigin	60	1.0024	1.0157	1.0138	1.4429	4.0778	**1.0000**
10	Rosenbrock	60	**1.0000**	363.4367	**1.0000**	44,236.6667	52.6500	**1.0000**
Average			1.2829	110.2952	8.3344	12,069.8681	235.9944	4.6352
Standard deviation			0.5076	200.5849	18.2363	24,719.6405	465.7421	4.8015

The symbol bold represents the best value which is normalized to 1 in each case.

Table 18 Summarized normalized average MARE values for all benchmark problems

ndes	*ntest*	*ntotal*	EM-MROWF	GOEL	ACAR	PRS	RBF	KRG
20	1000	1020	1.2185	2.0746	2.2251	9.4320	6.1034	**1.0000**
30	1000	1030	**1.0000**	4.7806	4.1481	91.0848	26.2443	1.2709
40	1000	1040	**1.0000**	15.8639	2.1654	853.3269	32.3197	11.8702
50	1000	1050	**1.0000**	19.4058	3.6045	1793.9642	22.3338	12.3697
60	1000	1060	**1.0000**	85.9733	6.4965	9408.2688	183.9539	3.6131
Average			1.0437	25.6196	3.7279	2431.2154	54.1910	6.0248
Standard deviation			0.0874	30.8707	1.5847	3547.2903	65.4600	5.0615

The symbol bold represents the best value which is normalized to 1 in each case.

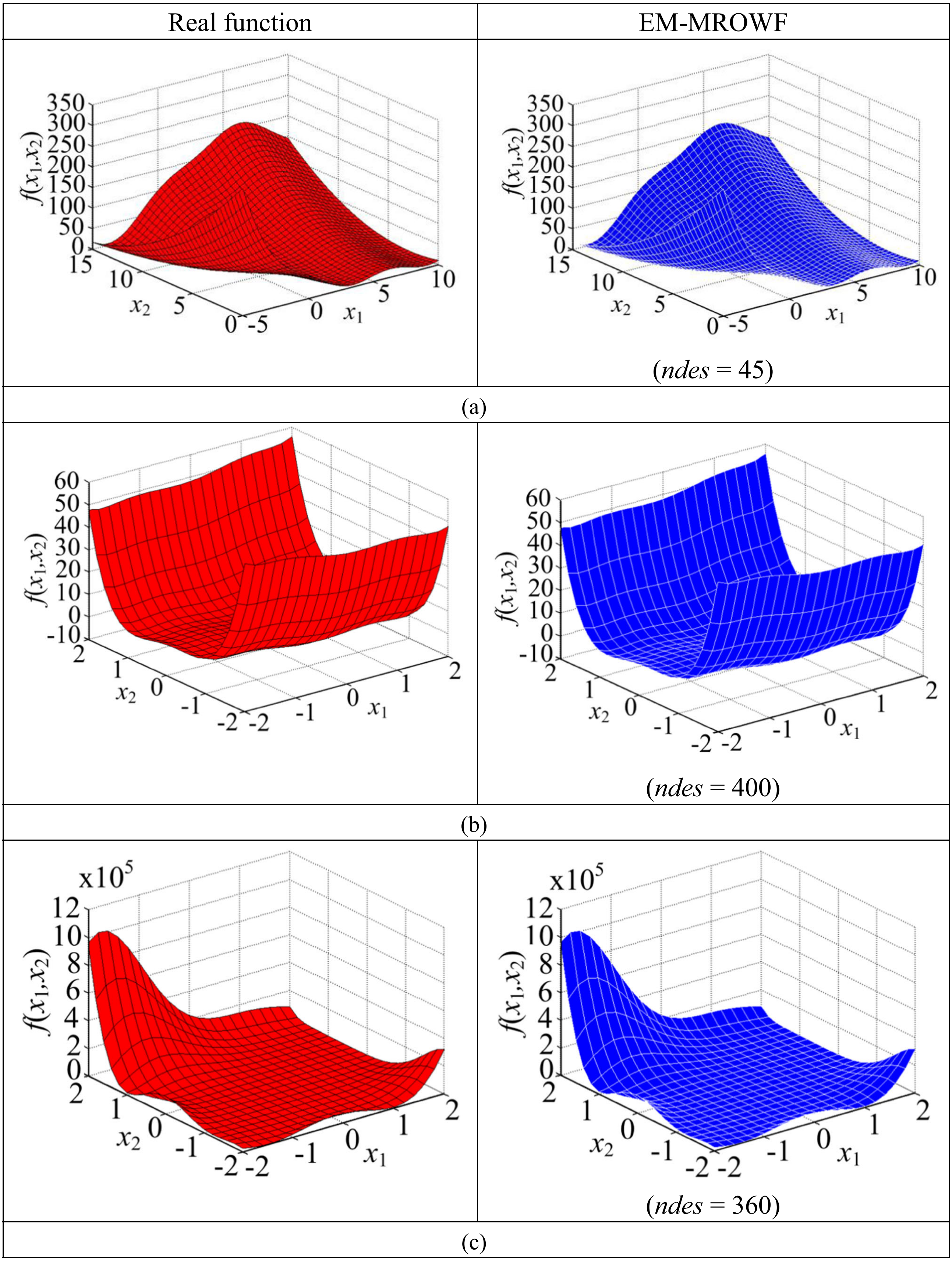

Fig. 6 Plots of benchmark functions: (**a**) Branin-Hoo, (**b**) Camelback, (**c**) Goldstein-price, (**d**) 2-D Multi-modal, (**e**) Rosenbrock, (**f**) Haupt, (**g**) Crane, (**h**) Peak, (**i**) Waving, (**j**) Rastrigin

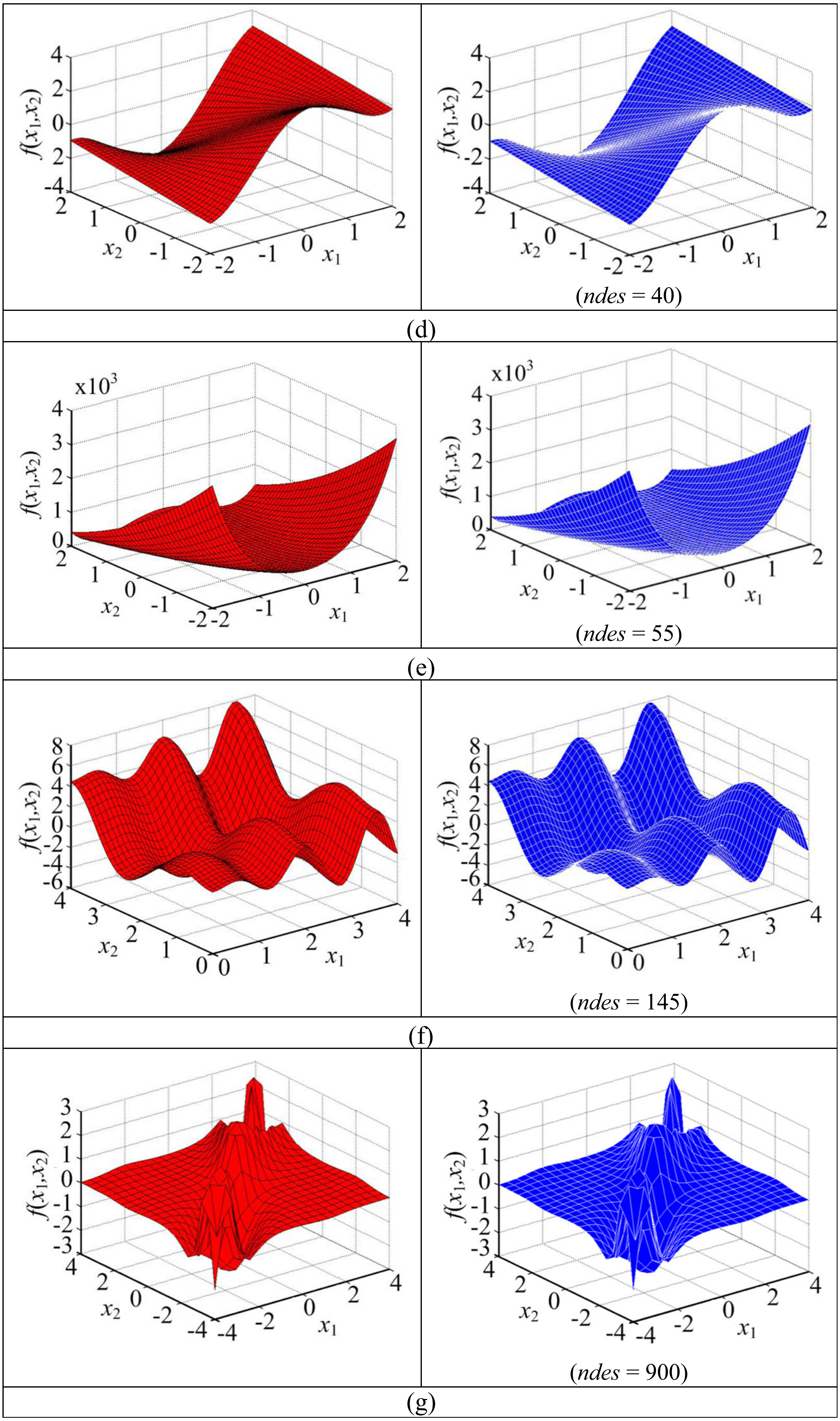

Fig. 6 (continued)

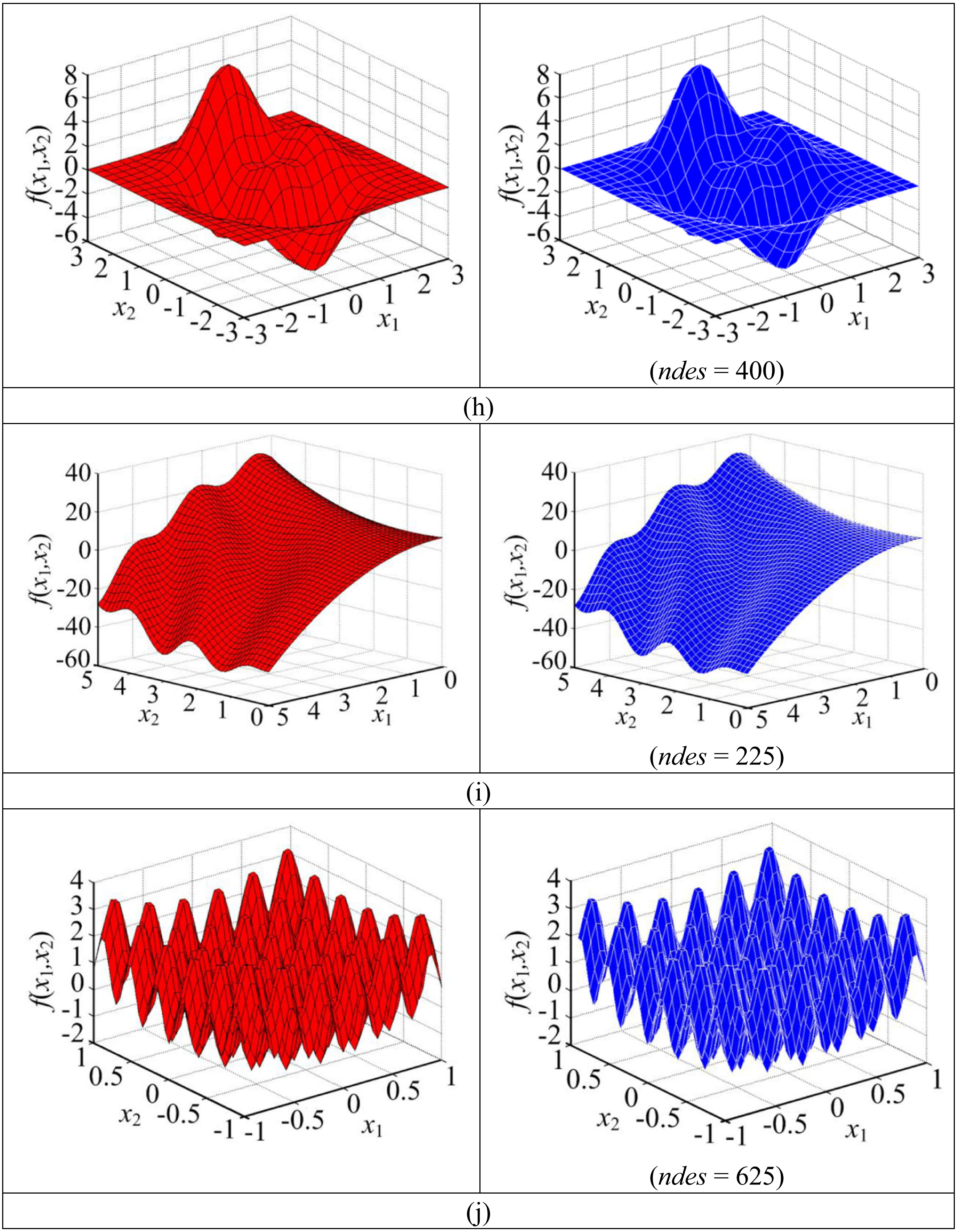

Fig. 6 (continued)

Table 19 Normalized RMSE values for Test 2

ID	*nvar*	*ndes*	*ntest*	*ntotal*	EM-MROWF	GOEL	ACAR	PRS	RBF	KRG
1	3	90	1000	1090	**1.0000**	1.0607	1.0756	6.8580	1.4900	1.0756
2	4	120	1000	1120	**1.0000**	1.1408	1.0017	1.7377	1.0017	2.2586
3	5	150	1000	1150	**1.0000**	1.0056	1.0041	1.1078	1.0698	1.5154
4	6	180	1000	1180	**1.0000**	1.0256	1.0130	1.1234	1.1641	1.7998
5	7	210	1000	1210	**1.0000**	1.0061	1.0334	1.1246	1.1125	1.7432
6	8	240	1000	1240	**1.0000**	1.0507	1.0162	1.0904	1.1562	1.9385
Average					1.0000	1.0483	1.0240	2.1736	1.1657	1.7219
Standard deviation					0.0000	0.0462	0.0253	2.1074	0.1550	0.3656

The symbol bold represents the best value which is normalized to 1 in each case.

of the cross section (R) and wall thickness (t), as illustrated in Fig. 4b. In this study, the ranges of the design variables were chosen as [60 mm, 100 mm] and [1 mm, 3 mm] for R and t, respectively. Using numerical simulations, the three responses, EA, PCF and SEA, were obtained for design points and test points, as given in Tables 2 and 3, respectively. The metamodels of the three responses are established in the next section.

4.2.2 Airbag cushion problem

Airbag is recognized as effective cushion equipment and is now widely used for the occupant protection in vehicles. In this study, the FE model of a driver's airbag, as shown in Fig. 5, was created by LS-DYNA (Hallquist 1998a, b) and used to simulate the impact between the driver's head and the airbag. In the driver's airbag system, the mass of the inflation gas and the vent area have a big effect on the cushion property. In order to investigate the cushion property of the driver's airbag, the peak acceleration a_{peak} of the head was employed as the indicator. The input mass of the inflation gas and the vent area were chosen as the design variables. In this work, the input mass of the inflation gas of a standard driver's airbag (LS-PrePost Online Document 2012) was scaled by a parameter λ which changed from 0.5 to 1.5. The vent area A changed from 0 to 628 mm^2 (i.e. the radiuses of the two vent holes of the airbag were from 0 to 10 mm). Using FE simulations, the responses a_{peak} were obtained for design points and test points, as given in Tables 4 and 5, respectively. The metamodel of the response is established in the next section.

5 Results and discussion

In this section, the EMs and the individual metamodels (i.e., PR, RBF and KRG) for the benchmark problems, thin-walled column crash problem and airbag cushion problem were constructed. To evaluate to prediction performances, RMSE and MARE values were calculated using the test points.

5.1 Benchmark problems

5.1.1 Test 1: Prediction performance with various number of design points

In order to compare the prediction performance of the EMs and the individual metamodels, the normalized RMSE and MARE values of these metamodels with different number of design points for the ten benchmark problems were calculated using (9) and (10), respectively. The numbers of the design points and test points generated for these benchmark problems were summarized in Table 6. In this test, the number of design points *ndes* was set to 20, 30, 40, 50 and 60, the corresponding normalized RMSE results were listed in Tables 7, 8, 9, 10 and

Table 20 Normalized MARE values for Test 2

ID	*nvar*	*ndes*	*ntest*	*ntotal*	EM-MROWF	GOEL	ACAR	PRS	RBF	KRG
1	3	90	1000	1090	**1.0000**	1.6021	4.7891	184.0687	6.0928	4.7891
2	4	120	1000	1120	**1.0000**	2.4451	1.0000	17.2275	**1.0000**	2.7933
3	5	150	1000	1150	**1.0000**	1.2381	1.2697	1.8374	**1.0000**	1.2811
4	6	180	1000	1180	**1.0000**	1.9379	1.5761	2.8941	**1.0000**	2.4218
5	7	210	1000	1210	**1.0000**	1.2166	1.1830	1.3739	1.3251	1.7689
6	8	240	1000	1240	**1.0000**	1.1849	1.1635	2.3255	1.6223	3.0165
Average					1.0000	1.6041	1.8302	34.9545	2.0067	2.6784
Standard deviation					0.0000	0.4616	1.3346	66.9156	1.8416	1.1127

The symbol bold represents the best value which is normalized to 1 in each case.

Table 21 Normalized RMSE values for the engineering application problems

ID	Response	*nvar*	*ndes*	*ntest*	*ntotal*	EM-MROWF	GOEL	ACAR	PRS	RBF	KRG
1	SEA	2	20	20	40	**1.0000**	1.1952	1.1459	1.1459	1.9799	1.0457
2	EA	2	20	20	40	**1.0000**	1.2412	1.2431	1.5259	2.6747	1.2736
3	PCF	2	20	20	40	**1.0000**	1.0241	1.0561	1.2422	1.2123	1.0304
4	a_{peak}	2	20	20	40	**1.0000**	1.0250	1.0242	1.0341	1.0517	1.0055
Average						1.0000	1.1214	1.1173	1.2370	1.7297	1.0888
Standard deviation						0.0000	0.0982	0.0852	0.1823	0.6487	0.1076

The symbol bold represents the best value which is normalized to 1 in each case.

11, respectively. And, the normalized average RMSE values for the ten benchmark problems were summarized in Table 12. All the RMSE values listed in these tables were normalized by setting the best (the lowest) value to 1. In each table, the overall performance for all 10 test problems was estimated using the average normalized RMSE value shown in the penultimate row. Generally, the smaller the average normalized RMSE, the better the overall performance of the metamodel. In addition, in each table, the standard deviations of the three kinds of the EMs were calculated and given in the last row of the table. As we know, the smaller the standard deviation, the more robust the performance of the metamodel. In addition, the normalized MARE results for the cases of *ndes* = 20, 30, 40, 50 and 60 were given in Tables 13, 14, 15, 16 and 17, respectively. The normalized average MARE values for the ten benchmark problems were summarized in Table 18.

From Table 7 and Table 13, it can be found that the average value and the standard deviation of EM-MROWF for the case of *ndes* = 20 both were the second-smallest for the normalized RMSE and MARE, respectively. And, from Table 8 and Table 14, Table 9 and Table 15, Table 10 and Table 16, and Table 11 and Table 17, the average value and the standard deviation of EM-MROWF for the cases of *ndes* = 30, 40, 50 and 60 both were the smallest for the normalized RMSE and MARE. From the summarized results given in Table 12 and Table 18, it can be seen that EM-MROWF performed best in 4 cases out of 5 test cases for all the ten benchmark problems. In addition, from Table 12 and Table 18, we found that the average value and the standard deviation of EM-MROWF both were the smallest for the normalized RMSE and MARE, respectively. Generally, from the comparison results of Test 1, it can be found that the proposed EM-MROWF was the most accurate and robust metamodel for the ten benchmark problems.

It should be pointed out that the adjacent region of the EM-MROWF is not strictly continuous, but there is a transition process for two adjacent regions in this study. The weight factors of the adjacent region were set as the average values of the weight factors of the two adjacent regions. Thus, the transition of the two adjacent regions was relatively smooth. Figure 6 shows the plots of the real functions and the response surfaces of the proposed EMs for the benchmark functions. From each Figure, it can be seen that the response surface of the EM-MROWF (*ndes* was chosen as the value when the metamodel was accurate enough) agreed with the real function well and the transition of the adjacent regions was smooth. Thus, the adjacent region of the EM-MROWF performed well.

5.1.2 Test 2: Prediction performance with various number of design variables

In order to compare the prediction performance of the EMs described in Sections 2 and 3 as *nvar* varied, normalized values of the EMs and the individual metamodels for the Rosenbrock function (20) with different *nvar* were calculated using (9) and (10). In this test, *nvar* was set to 3, 4, 5, 6, 7 and 8. The number of the design points *ndes* was set to 30*nvar*. The results of Test 2 are summarized in Table 19 and Table 20. All the RMSE and MARE values listed in

Table 22 Normalized MARE values for the engineering application problems

ID	Response	*nvar*	*ndes*	*ntest*	*ntotal*	EM-MROWF	GOEL	ACAR	PRS	RBF	KRG
1	SEA	2	20	20	40	**1.0000**	1.5334	1.2751	1.2751	3.6687	1.4179
2	EA	2	20	20	40	**1.0000**	4.6280	4.4653	4.4653	7.8274	3.7270
3	PCF	2	20	20	40	1.1820	**1.0000**	1.1820	1.1505	1.1982	1.7096
4	a_{peak}	2	20	20	40	**1.0000**	1.0381	1.0364	1.0495	1.0455	**1.0000**
Average						1.0455	2.0499	1.9897	1.9851	3.4350	1.9636
Standard deviation						0.0788	1.5033	1.4318	1.4342	2.7414	1.0489

The symbol bold represents the best value which is normalized to 1 in each case.

Tables 19 and 20 were normalized by setting the best (the lowest) value to one. From Tables 19 and 20, it can be seen that the proposed EM-MROWF was the most accurate and robust metamodel for Test 2.

5.2 Engineering application problems

Tables 21 and 22 summarizes the normalized RMSEs and MAREs of the EMs as well as the individual metamodels for the three responses (SEA, EA and PCF) of the thin-walled column crash problem and one response (the peak acceleration a_{peak}) of the head in the airbag cushion problem, respectively. From Table 21, EM-MROWF had the best prediction performance in 4 cases. And, from Table 22, out of the 4 cases, EM-MROWF had the best prediction performance in 3 cases. Based on the average normalized RMSE and MARE shown in the penultimate row of Tables 21 and 22, we found that the overall prediction performance of EM-MROWF was the best for the two engineering application problems. As shown in the last row of Tables 21 and 22, the standard deviation of EM-MROWF was found to be the smallest. This indicated that EM-MROWF was the most robust one among the investigated metamodels. Therefore, based on the comparison results of the two engineering application problems, it was found that the accuracy and the robustness of EM-MROWF was the best.

In a word, it can be found that EM-MROWF was the most accurate and robust EM among the three average ensemble of metamodels and the three individual metamodels for the benchmark problems as well as the engineering application problems.

6 Conclusions

In this study, a new ensemble of metamodels (EM), i.e., EM with multiple regional optimized weight factors (EM-MROWF), was proposed and evaluated. This new EM is different from the commonly used EMs in which it divides the design space into subdomains and assigns each subdomain with a set of optimized weight factors. In each of the divided region, a set of optimized weight factors is determined by minimizing the GMSE in that region. Ten benchmark problems and two engineering application problems (i.e., a thin-walled column crash problem and an airbag cushion problem) were employed to evaluate the prediction performance of the EM-MROWF.

In order to show the usefulness of the EM-MROWF, the prediction performance of EM-MROWF was compared to those of the two existing EMs and the individual metamodels. All the comparison results for the ten benchmark problems and two engineering application problems showed that EM-MROWF had the best prediction performance for both accuracy and robustness. Thus, EM-MROWF was an effective metamodeling method and could be used in practical engineering.

Acknowledgments This work is supported jointly by the National Science Foundation for Young Scientists of China (No. 11302075), the National Science Fund for Distinguished Young Scholars of China (No. 11225212), the Natural Science Foundation of Hunan Province of China (No. 14JJ3061), and the Young Teacher Development Plan of Hunan University of China. The authors also would like to thank the support from the Collaborative Innovation Center of Intelligent New Energy Vehicle, and the Hunan Collaborative Innovation Center of Green Automobile.

References

Acar E (2010) Various approaches for constructing an ensemble of metamodels using local measures. Struct Multidiscip Optim 42(6): 879–896

Acar E (2015) Effect of error metrics on optimum weight factor selection for ensemble of metamodels. Expert Syst Appl 42(5):2703–2709

Acar E, Rais-Rohani M (2009) Ensemble of metamodels with optimized weight factors. Struct Multidiscip Optim 37(3):279–294

Bishop CM (1995) Neural networks for pattern recognition. Oxford University Press Inc., New York

Box GEP, Hunter WG, Hunter JS (1978) Statistics for experimenters. Wiley, New York

Buhmann MD (2003) Radial basis functions: theory and implementations. Cambridge University Press, New York

Clarke SM, Griebsch JH, Simpson TW (2005) Analysis of support vector regression for approximation of complex engineering analyses. J Mech Des 127(11):1077–1087

Diana LM, Dachuan TS, Victoria CPC, Seoung BK (2015) A convex version of multivariate adaptive regression splines. Comput Stat Data Anal 81:89–106

Dyn N, Levin D, Rippa S (1986) Numerical procedures for surface fitting of scattered data by radial basis functions. SIAM J Sci Stat Comput 7(2):639–659

Fang H, Rais-Rohani M, Liu Z, Horstemeyer MF (2005) A comparative study of metamodeling methods for multiobjective crashworthiness optimization. Comput Struct 83:2121–2136

Fang JG, Sun GY, Qiu N, Kim NH, Li Q (2017) On design optimization for structural crashworthiness and its state of the art. Struct Multidiscip Optim 55(3):1091–1119

Ferreira WG, Serpa AL (2016) Ensemble of metamodels: the augmented least squares approach. Struct Multidiscip Optim 53(5):1019–1046

Forrester AIJ, Keane AJ (2009) Recent advances in surrogate based optimization. Prog Aerosp Sci 45:50–79

Goel T, Haftka RT, Shyy W, Queipo NV (2007) Ensemble of surrogates. Struct Multidiscip Optim 33(3):199–216

Gu XG, Lu JW, Wang HZ (2015) Reliability-based design optimization for vehicle occupant protection system based on ensemble of metamodels. Struct Multidiscip Optim 51(2):533–546

Gunn SR (1997) Support vector machines for classification and regression. Technical Report, Image Speech and Intelligent Systems Research Group, University of Southampton, UK

Hallquist JO (1998a) LS-DYNA theoretical manual. Livemore Software Technology Corporation, California

Hallquist JO (1998b) LS-DYNA keyword user's manual. Livemore Software Technology Corporation, California

Hou SJ, Li Q, Long SY, Yang XJ, Li W (2007) Design optimization of regular hexagonal thin-walled columns with crashworthiness criteria. Finite Elem Anal Des 43(6–7):555–565

Jerome HF (1990) Multivariate dynamic regression splines. Technical Report 102, Stanford Linear Accelerator Center and Department of Statistics, Stanford University, USA

Jin R, Chen W, Simpson TW (2001) Comparative studies of metamodelling techniques under multiple modelling criteria. Struct Multidiscip Optim 23(1):1–13

Kim HS (2002) New extruded multi-cell aluminum profile for maximum crash energy absorption and weight efficiency. Thin Wall Struct 40(4):311–327

Lee Y, Dong-Hoon C (2014) Pointwise ensemble of metamodels using v nearest points cross-validation. Struct Multidiscip Optim 50:383–394

LS-PrePost Online Document (2012) http://www.lstc.com/lspp/content/tutorials/3/curves.k. California: Livemore Software Technology Corporation

MacKay DJC (1998) Introduction to Gaussian processes. In: Bishop CM (ed) Neural networks and machine learning. NATO ASI series, vol 168. Springer, Berlin, pp 133–165

Myers RH, Montgomery DC (2002) Response surface methodology: process and product optimization using designed experiments. Wiley, New York

Queipo NV, Haftka RT, Shyy W, Goel T, Vaidyanathan R, Tucker PK (2005) Surrogate-based analysis and optimization. Prog Aerosp Sci 41:1–28

Rasmussen CE, Williams CKI (2006) Gaussian processes for machine learning. The MIT Press, Cambridge

Sacks J, Welch WJ, Mitchell TJ, Wynn HP (1989) Design and analysis of computer experiments. Stat Sci 4(4):409–435

Sanchez E, Pintos S, Queipo NV (2008) Toward an optimal ensemble of kernel-based approximations with engineering applications. Struct Multidiscip Optim 36(3):247–261

Simpson TW, Mauery TM, Korte JJ, Mistree F (2001) Kriging models for global approximation in simulation-based multidisciplinary design optimization. AIAA J 39(12):2233–2241

Smith M (1993) Neural networks for statistical modeling. Von Nostrand Reinhold, New York

Song XG, Sun GY, Li GY, Gao WZ, Li Q (2013) Crashworthiness optimization of foam-filled tapered thin-walled structure using multiple surrogate models. Struct Multidiscip Optim 47(2):221–231

Wang GG, Shan S (2007) Review of metamodeling techniques in support of engineering design optimization. ASME J Mech Des 129(4):370–380

Wikipedia (2015) Test functions for optimization. https://en.wikipedia.org/wiki/Test_functions_for_optimization

Yin HF, Wen GL, Gan NF (2011) Crashworthiness design for honeycomb structure under axial dynamic loading. Int J Comput Methods 8(4):863–877

Yin HF, Wen GL, Fang HB, Qing QX, Kong XZ, Xiao JR, Liu ZB (2014) Multiobjective crashworthiness optimization design of functionally graded foam-filled tapered tube based on dynamic ensemble metamodel. Mater Des 55:747–757

Zerpa LE, Queipo NV, Pintos S, Salager J-L (2005) An optimization methodology of alkaline-surfactant-polymer flooding processes using field scale numerical simulation and multiple surrogates. J Pet Sci Eng 47:197–208

Zhang J, Chowdhury S, Messac A (2012) An adaptive hybrid surrogate model. Struct Multidiscip Optim 46(2):223–238

Zhou XJ, Jiang T (2016) Metamodel selection based on stepwise regression. Struct Multidiscip Optim 54(3):641–657

Zhou XJ, Ma YZ, Li XF (2011) Ensemble of surrogates with recursive arithmetic average. Struct Multidiscip Optim 44(5):651–671